

## Effects of environmental conditions on the seasonal distribution of phytoplankton biomass in the North Sea

*M. Llope*<sup>1</sup>

Centre for Ecological and Evolutionary Synthesis (CEES), Department of Biology, University of Oslo, P.O. Box 1066 Blindern, N-0316 Oslo, Norway

Sir Alister Hardy Foundation for Ocean Science (SAHFOS), The Laboratory, Citadel Hill, Plymouth, PL1 2PB, United Kingdom

*K.-S. Chan*

Department of Statistics and Actuarial Science, University of Iowa, 263 Schaeffer Hall, Iowa City, Iowa 52242

*L. Ciannelli*

College of Oceanic and Atmospheric Sciences, Oregon State University, Corvallis, Oregon 97331

*P. C. Reid*

University of Plymouth, Marine Institute, Drake Circus, Plymouth, PL4 8AA, United Kingdom

Sir Alister Hardy Foundation for Ocean Science (SAHFOS), The Laboratory, Citadel Hill, Plymouth, PL1 2PB, United Kingdom

*L. C. Stige*

Centre for Ecological and Evolutionary Synthesis (CEES), Department of Biology, University of Oslo, P.O. Box 1066 Blindern, N-0316 Oslo, Norway

*N. C. Stenseth*

Centre for Ecological and Evolutionary Synthesis (CEES), Department of Biology, University of Oslo, P.O. Box 1066 Blindern, N-0316 Oslo, Norway

Flødevigen Marine Research Station, Institute of Marine Research, N-4817 His, Norway

### *Abstract*

We study the spatial and seasonal variability of phytoplankton biomass (as phytoplankton color) in relation to the environmental conditions in the North Sea using data from the Continuous Plankton Recorder survey. By using only environmental fields and location as predictor variables we developed a nonparametric model (generalized additive model) to empirically explore how key environmental factors modulate the spatio-temporal patterns of the seasonal cycle of algal biomass as well as how these relate to the ~1988 North Sea regime shift. Solar radiation, as manifest through changes of sea surface temperature (SST), was a key factor not only in the seasonal cycle but also as a driver of the shift. The pronounced increase in SST and in wind speed after the 1980s resulted in an extension of the season favorable for phytoplankton growth. Nutrients appeared to be unimportant as explanatory variables for the observed spatio-temporal pattern, implying that they were not generally limiting factors. Under the new climatic regime the carrying capacity of the whole system has been increased and the southern North Sea, where the environmental changes have been more pronounced, reached a new maximum.

---

<sup>1</sup> Corresponding author (marcos.llope@bio.uio.no).

### *Acknowledgments*

We thank the many people, including past and present Continuous Plankton Recorder (CPR) workers, whose efforts helped to establish and maintain the database presented here, and the international funding consortium that support the CPR survey. Helpful discussions with Robin D. Pingree, Priscilla Licandro, and Martin Edwards on the functioning of the North Sea system are much appreciated. Doug Beare and Abigail McQuatters-Gollop kindly helped to put together the environmental database. We also wish to thank two anonymous reviewers for their helpful comments and suggestions. This work was supported by a postdoctoral grant from the Ministerio de Educación y Ciencia (EX2006-0650, MEC Postdoctoral Fellowship) and a Marie Curie Intra-European fellowship (FP6-2005-Mobility-5, European Commission). KSC and LC gratefully acknowledge partial support from the U.S. National Science Foundation and the North Pacific Research Board. LCS thanks the Norwegian Research Council for support.

Climate change is one of the most important environmental issues that the Earth, and the ocean in particular, are facing this century (Intergovernmental Panel on Climate Change 2007). In order to better adapt to the consequences of climate change on the ocean, improved knowledge of how climate controls the base of marine food webs is needed, because this is the first level of interaction between climate and ecosystems. One way to gather such knowledge is by developing statistical models able to reproduce the observed dynamics of phytoplankton. Such models enable an evaluation of how the environment regulates the productivity of marine systems and, in due course, how the entire ecosystem might be affected.

Long-term biological data are essential for this purpose and must also have sufficient spatial extent to detect different regional responses. The Continuous Plankton Recorder (CPR) survey is the only long-term biological monitoring program that gives a systematic coverage of the

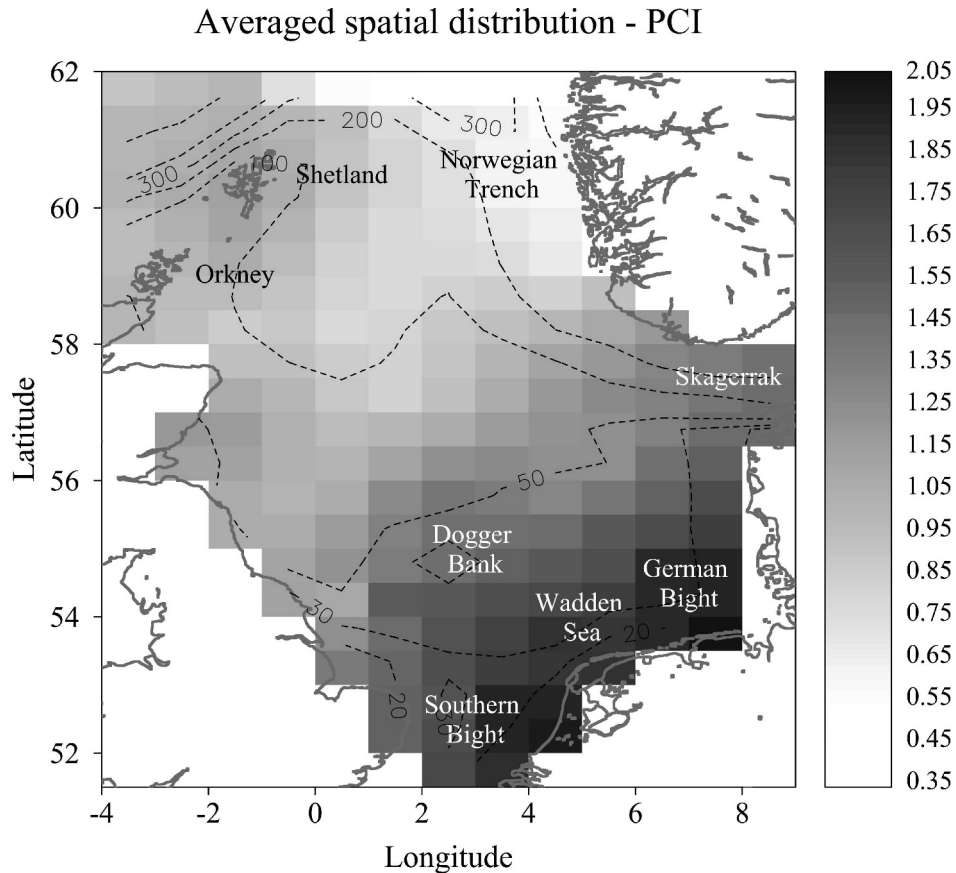


Fig. 1. The North Sea PCI. Spatial distribution of the annual-averaged Phytoplankton Colour Index (PCI) in the North Sea from WinCPR (version 1.1). The data grid is based on a Mercator projection of a half-degree latitude  $\times$  1° longitude and, thus, not a 1 : 1 equal area projection. The names of the different areas are shown.

North Sea in space and time (Edwards et al. 2001). In this study we focus on the Phytoplankton Colour Index (PCI), a semi-quantitative in situ measurement of surface phytoplankton biomass, with a methodology that has remained consistent since at least 1948 (Reid et al. 2003).

Despite its relatively small size, the North Sea (Fig. 1) shows great geographic variability due to the combination of both a highly enclosed location (which enhances the continental influence) and a changing bathymetry. This, as illustrated in Fig. 1, results in a rich toponymy, unlike many other seas where the different areas are referred to by alluding to their geographic location (south, north, northeast, etc.). For the most part, the sea lies on the European continental shelf, being relatively shallow in the south (<50 m). In the central-south, extensive sandbanks are found on the Dogger Bank. A sandy, shallow bottom together with a location in the middle of the sea away from coastal influence ensures that Dogger Bank waters are clear, particularly when compared to the turbid coastal regions of the German Bight, Wadden Sea, and Southern Bight. To the north, beyond the Orkney Islands and Shetlands Isles, the North Sea opens to the eastern North Atlantic. On its eastern margin the Norwegian Trench extends down to >300 m and opens in a widening funnel shape to the Norwegian Sea, and in the south via the Skagerrak to the Baltic Sea. This great bathymetric and

geographic heterogeneity is reflected in its hydrography and in turn in plankton abundance and distribution (*see* PCI climatology in the Web Appendix, [www.aslo.org/lo/toc/vol\\_54/issue\\_2/0512a.pdf](http://www.aslo.org/lo/toc/vol_54/issue_2/0512a.pdf)), making the North Sea a challenging ecosystem to study and to model.

The North Sea also provides a unique example of an ecological regime shift recorded over a large area (Reid et al. 2001). This abrupt change, which took place in the late eighties, was first described for the phytoplankton using the same PCI database as for this study (Reid et al. 1998). The description, causes, and consequences of this shift have generated an extensive body of literature (*see* review by Beaugrand 2004). However, to our knowledge, none of these studies have focused on the relative importance of different environmental forcing mechanisms at the same time as explicitly including a spatial perspective. To explain the causal links leading to the biological shift a new modeling approach to the CPR data has been applied in this study. The aim was to develop a statistical model capable of reproducing the observed spatial pattern of the PCI seasonal cycle in the North Sea and at the same time use the statistically derived insight to deduce the structuring effects of the environment. The analysis of changes in environment–phytoplankton interactions was divided in three parts: (1) The annual cycle was modeled based on all the historical data (1948–2004), including location and

environment as predictors. This spatio-environmental model was used to explore how mean environmental conditions regulate the seasonal cycle of phytoplankton. (2) The model output was then compared to two new model runs, one including only spatio-temporal and the other only environmental variables. (3) Repeating the same analysis as for 1, we approached the regime shift issue by dividing the whole series into two periods, pre- and post-regime shift.

## Methods

*The Phytoplankton Colour Index*—The PCI is an estimate of phytoplankton biomass that is based on the color that the accumulation of green chlorophyll pigments gives to the CPR filtering silk (Batten et al. 2003a). As such, PCI is a unique measurement of phytoplankton biomass, because small phytoplankton cells (e.g., unarmored flagellates, which tend to disintegrate when they contact formaldehyde) that cannot be counted under the microscope contribute to the coloration of the filtering silk (Batten et al. 2003b). Although it is a good general biomass proxy (representing the standing stock, not primary production rate), it cannot be used to distinguish between the relative abundance of diatoms and dinoflagellates over time.

The PCI is a categorical index determined on the silk by reference to a four-rank standard color chart. These four categories of PCI are then assigned numerical values (0, 1, 2, 6.5) on a ratio scale based on acetone extracts (Colebrook and Robinson 1965). Although it is a proxy for chlorophyll, the PCI is not a proper chlorophyll measure. Because this is not a mechanized method, but done by analysts, there might be some degree of subjectivity. Also, its 'semi-quantitative' condition with a large difference between the top category (6.5) and the next one (2) might make interpretation of the data difficult at times. Nevertheless, two separate comparisons between the PCI and surface chlorophyll *a* (Chl *a*) estimated by the SeaWiFS satellite, showed good agreement (Raitzos et al. 2005; McQuatters-Gollop et al. 2007). Most importantly, the PCI is the only long-term proxy for algal biomass going back to the late 1940s, long before accurate satellite measurements started in 1997 (i.e., SeaWiFS).

The PCI was extracted directly from WinCPR (version 1.1; Sir Alister Hardy Foundation for Ocean Science), a software package that provides a gridded integration of CPR data for the North Sea on 183 pixels, each one covering an area of 1° longitude by 0.5° latitude (<http://cpr.network-research-group.org/>). Full details of the operation of the CPR have been published extensively elsewhere (Batten et al. 2003a). The WinCPR gridded spatial interpolation was performed using the Inverse Square Distance method (ISD). This implies that the weights of the samples used to calculate each pixel value are inversely proportional to the squared distance from the point being estimated. The ISD parameters were optimized for the North Sea to find the best compromise between the number of CPR samples per month and the need to keep the missing pixels to a minimum. Briefly, the maximum distance was selected at 162 nautical miles and the minimum number of neighbors used in the estimation of

each pixel was set to 5 and the maximum to 15. The accuracy of the interpolation was validated through a comparison with previous analysis of CPR data (Vezzulli et al. 2007). The advantages of using a gridded database are obvious; however, it has also disadvantages, the most important of them being the spatial dependency of the samples (*see* The analysis). The time series (1948–2004) were averaged per month in order to get the seasonal distribution (12 months) for the 182 pixels (pixel 87 was not used because it contained no information). For the pre- and post-shift models, the seasonal averages were calculated using the values either before or after (and including) year 1988, because this is the year when the shift occurred in PCI (Reid et al. 1998; Beaugrand 2004). The total number of samples used in the WinCPR calculation ranged from ~700 samples to ~1300 samples per year. The total number of samples during the two periods was: 38,632 samples for the preshift (1948–1987; 40 yr) and 15,928 for the post-shift (1988–2004; 17 yr), which gives a very similar average number of samples per year, 966 and 937 pre- and post-shift respectively. Therefore, the sampling intensity can be considered as balanced over the two periods.

*The variables*—Sea surface temperature (SST; °C) data were obtained from the British Atmospheric Data Centre; HadISST 1.1 dataset (<http://badc.nerc.ac.uk/home/>). Surface downward solar radiation flux (SOL; W m<sup>-2</sup>) and wind speed (WND; m s<sup>-1</sup>) data (National Centers for Environmental Prediction Reanalysis data set) were obtained from National Oceanic and Atmospheric Administration/Office of Oceanic and Atmospheric Research/Earth System Research Laboratory Physical Sciences Division, from their web site at <http://www.cdc.noaa.gov/>. The solar radiation flux was estimated at the bottom of the atmosphere (Kalnay et al. 1996) and, therefore, is considered as the radiation received at the Earth's surface (taking into account calculated cloud coverage). These three variables consisted of a gridded time series matching the PCI time span (1948–2004).

Mixed layer depth (MLD) data were obtained from the project Ocean Mixed Layer Depth Climatology (<http://www.lodyc.jussieu.fr/~cdblod/mld.html>). The MLD has been calculated based on high vertical-resolution hydrographic profiles available since 1941 through 2002 (Montégut et al. 2004). The nitrate (NO<sub>3</sub>) climatology was calculated using field observations from the International Council for the Exploration of the Sea (ICES) Oceanographic Database (<http://www.ices.dk/ocean/>) covering the period 1960–2006. Both MLD and NO<sub>3</sub> climatologies include observations before and after the shift and overlap well the CPR temporal span (1948–2004).

Apart from these variables, which were input to the models, some others (*see* below) were also tested, but not used because they were not significant. These included bathymetry from the General Bathymetric Chart of the Oceans (<http://www.ngdc.noaa.gov/mgg/gebco/gebco.html>), the Simpson Hunter stratification parameter (a proxy for tidal-induced turbulence) from Pingree and Griffiths (1978) and phosphate concentration from the ICES Database.

Table 1. Generalized Additive Model (GAM) results. Intercept, estimated degrees of freedom (edf) and significance ( $p$ -value) of the spatial and environmental covariates for the whole-series, preshift, and post-shift GAMs. The  $p$ -values (and standard errors of the intercept) were calculated from bootstrapping. Although the number of edf for wind speed in the whole-series model is one of the highest, suggesting a strong nonlinear response to this variable, the partial residual plot (Fig. 2) indicates that its effect is monotonically increasing and nearly linear. But constraining the wind effect to be linear yields a slightly worse fit ( $R^2 = 0.861$ ; generalized cross-validation [GCV] score: 0.0184), so the original variable was retained.

	Whole-series		Preshift		Post-shift	
	Estimate	$p$ -value	Estimate	$p$ -value	Estimate	$p$ -value
Intercept	0.7096	<0.001	0.6060	<0.001	0.9171	<0.001
SE	$\pm 0.0084$		$\pm 0.0110$		$\pm 0.0091$	
	edf	$p$ -value	edf	$p$ -value	edf	$p$ -value
(Long, Lat)	27.062	<0.001	21.419	<0.001	23.465	<0.001
SOL*	4.000	<0.001	4.000	<0.001	3.929	<0.001
SST†	3.854	<0.001	3.906	<0.001	3.768	<0.001
MLD‡	3.977	<0.001	3.988	<0.001	3.918	<0.001
WND§	3.747	0.024	3.640	0.021	-	-
NO3	3.635	0.028	3.840	0.082	3.533	0.003
	$R^2=0.862$		$R^2=0.820$		$R^2=0.858$	
	GCV=0.0183		GCV=0.0250		GCV=0.0198	

\* Solar radiation flux.

† Sea surface temperature.

‡ Mixed layer depth.

§ Wind speed.

|| Nitrate.

All the environmental variables were spatially interpolated to the same pixels used in WinCPR (1.1) and subsequently averaged by month (when it was not already a climatology) in the same way as was done with the PCI data.

*The analysis*—To build the seasonal model we used the PCI as a response variable, with covariates being the grid sample position (defined by longitude and latitude) as well as the different environmental variables (described above). Because no lag was used, the PCI was regressed against the monthly environmental conditions. The regression analysis was performed using nonparametric Generalized Additive Models (GAM; Hastie and Tibshirani 1990; Wood 2006) as used in Stenseth et al. (2006).

Specifically, let  $PCI_{m,(\lambda,\varphi)}$  be the log + 1-transformed PCI at longitude  $\lambda$  and latitude  $\varphi$  for the 12 months ( $m$ ), and SOL, SST, WND, MLD, and NO3 the co-located environmental variables to give the following model:

$$\begin{aligned}
 PCI_{m,(\lambda,\varphi)} = & a + s(\lambda,\varphi) + g_1 [SOL_{m,(\lambda,\varphi)}] + g_2 [SST_{m,(\lambda,\varphi)}] \\
 & + g_3 [MLD_{m,(\lambda,\varphi)}] + g_4 [WND_{m,(\lambda,\varphi)}] \\
 & + g_5 [NO3_{m,(\lambda,\varphi)}] + e_{m,(\lambda,\varphi)}
 \end{aligned} \quad (1)$$

where  $a$  is an intercept,  $s$  and  $g_s$  are nonparametric smooth functions (two-dimensional and one-dimensional respectively) describing the effect of location and environment on the PCI, and  $e_{m,(\lambda,\varphi)}$  is a random error assumed to be normally distributed with zero mean and finite variance. The two-dimensional (or spatial) effect was fitted with thin plate splines while the one-dimensional effects were fitted by natural cubic splines (Wood 2006).

Model selection was based on a stepwise approach, aimed at removing covariates with a  $p$ -value  $> 0.05$  and minimizing the generalized cross-validation (GCV) criterion of the model (Wood 2000). The GCV criterion is a measure of the out-of-sample predictive performance of the model, and it is related to Akaike's Information Criterion (AIC; Wood 2006).

The above formulation corresponds to the best spatio-environmental model, in which all predictor variables had significant effects (*see* Table 1). Apart from these variables, the surface concentration of phosphate, the bottom depth, and the degree of tidal mixing were tested but excluded because they did not prove to be significant in the model.

The residuals did not show temporal dependency but were spatially correlated. This results in an overestimation of the significance level of the covariates and, therefore, invalidates the standard  $p$ -values. To get an accurate estimate, the latter were computed using a wild bootstrap approach (Mammen 1993) which accounted for the spatial autocorrelation. Specifically, for a given fitted model: (1) the residuals were extracted, (2) rescaled, to have the same variance as the estimated scale parameter of the model, (3) their signs randomly inverted before being (4) used as a response variable in a model (having the same set of covariates as the original model), and finally (5) steps 3–4 were repeated 1000 times. To account for the spatial correlation, all residuals for a given month in a given bootstrap sample were either inverted or not with probability 0.5 (Davison and Hinkley 1997). We thus obtained a reference distribution of the  $F$ -ratio for each covariate for the null scenario of no covariate effects. The bootstrap estimate of the  $p$ -value for a covariate was calculated as the percentage of the reference  $F$ -ratios (out of the 1000 bootstrapped  $F$ -ratios) that were larger than the

observed  $F$ -ratio. Confidence limits for the partial effects of the covariates were calculated similarly to above, except that the rescaled and randomly inverted residuals were added back to the fitted values before fitting the model in step 4.

An alternative to using wild bootstrap is to incorporate the spatial correlation in the model. This approach, however, suffers from two difficulties: the spatial correlation structure is often unknown and hard to specify empirically, and the required statistical methodologies for model fitting and diagnostics are still undergoing intensive development and are not ready for application (Wood 2006). Fortunately, the objects of interest here are the additive regression effects. The spatial correlation is a nuisance feature whose omission from the model does not bias the estimation of the additive regression effects but only requires the wild bootstrap to validate their inference.

As explained in the introduction three sets of models were run: (1) whole-series, (2) preshift, and (3) post-shift. For the first model, average climatologies were calculated for the whole study period (1948–2004). For the latter two models, the original datasets were split into two periods: preshift (1948–1987; 40 yr) and post-shift (1988–2004; 17 yr) from which the spatial climatologies were subsequently calculated. For the depth of the mixed layer and the nutrients it was not possible to get preshift and post-shift climatologies with the same spatial resolution due to a lack of data. Therefore, the same climatology was retained for these variables in all the models. Note that by doing so we are assuming that these two variables have remained constant over the years. However, because we lack any other information, fixing these effects is the best approach to explore differences in the variables that can be shown to change over the two periods.

To evaluate the suitability of this modeling approach (which combines geographic and environmental variables, as specified in formula 1) to reproduce complex spatial patterns, we compared it with two alternative model formulations (formulas 2 and 3). Formula 2 describes a spatio-temporal model that includes the effect of location (i.e., the spatial effect) and 12 monthly factors as covariates (i.e., the intercept is allowed to change with the month). In this second formulation,  $M_i$  are the dummy variables for the 12 months and  $a_i$  are the monthly effects.

$$PCI_{m,(\lambda,\varphi)} = \sum_{i=1}^{12} a_i M_i + s(\lambda,\varphi) + e_{m,(\lambda,\varphi)} \quad (2)$$

Formula 3 describes an environmental model that incorporates all the climatological and physical variables, including depth (DEP) or tidal mixing (TID), but no geographical smoother (i.e., no spatial effect):

$$PCI_{m,(\lambda,\varphi)} = a + g_1 [SOL_{m,(\lambda,\varphi)}] + g_2 [SST_{m,(\lambda,\varphi)}] + g_3 [MLD_{m,(\lambda,\varphi)}] + g_4 [WND_{m,(\lambda,\varphi)}] + g_5 [NO3_{m,(\lambda,\varphi)}] + g_6 [DEP_{(\lambda,\varphi)}] + e_{m,(\lambda,\varphi)} \quad (3)$$

GAMs enjoy the advantage of being nonparametric (i.e., there is no need to a priori specify the functional forms

between the response and the explanatory variables), although it requires the covariate effects to be additive. This characteristic gives great flexibility to approximate the true relationships between the variables because we let the data tell us what these functional forms look like. Indeed, each function estimate is a natural cubic spline (Wood 2006; i.e., a function consisting of piecewise cubic polynomials pasted together so that the function is twice continuously differentiable, with the function itself being linear in the tails). The points where the cubic polynomials meet are called knots, the number of which generally increases with the sample size. Although the natural cubic spline function estimates can be written out in formulas, the formulas are hard to interpret and so, instead, the functions are plotted to reveal their general features. In summary, a fitted GAM has a very complex model formula that can be useful for computing fitted values and prediction, but, in terms of interpretation, it is best presented pictorially by plotting the graphs of its component functions. Often based on the estimated function shapes of a fitted GAM, a parametric model may be suggested. In the Web Appendix, a parametric approximation (second-order polynomial regression) is fitted and the coefficients are given because these could be useful for other authors.

All the calculations and models, including the processing of the variables and the plots, were coded in R (version 2.5.1; R Development Core Team 2007). The packages used were mgcv (Wood 2006) and RColorBrewer (Neuwirth 2007).

## Results

*Alternative formulations*—Using time and location as predictors (model formulation 2) is useful to produce summaries of the PCI but it tells us little about the causative mechanisms. The output from a purely environmental model (model formulation 3) is scientifically more meaningful but we usually do not have all the necessary independent variables to satisfactorily explain the observed dynamics. The spatio-environmental model (model formulation 1) provides a good compromise between the latter because the spatial term collects the variance not explained by the environmental conditions studied here. Moreover, a statistical comparison among them also supports the better performance of the spatio-environmental model. Specifically the  $R^2$  and GCV values of these models are both worse (lower and higher, respectively) than the  $R^2$  and GCV of the selected model shown in Table 1 (spatio-temporal model:  $R^2 = 0.79$ , GCV = 0.028, environmental model:  $R^2 = 0.71$ , GCV = 0.038). Therefore, the results showed in this section come from the spatio-environmental model.

However, the information provided by the alternative ‘pure’ models is also informative, particularly for comparison purposes, and can be found in the Web Appendix. It is worth mentioning that when the spatial smoother is not used, the bottom depth or the degree of tidal mixing become significant in the model. This could be seen as an indication that the spatial baseline is, to some degree, accounting for these effects (and others not explored).

Table 2. Variance contribution of the covariates. Coefficient of determination ( $R^2$ ), general cross validation score (GCV) and percentage of variance (%) accounted by the different models after deletion of one covariate. The left columns show these values for the models after stepwise deletion of the covariates listed to the left (first NO<sub>3</sub>, then WND, etc.). The last two models included only one variable: either space or SOL. For the right columns one covariate (those listed to the left) was removed at a time while keeping all the rest (i.e., with replacement).

	Stepwise deletion			Delete-one-covariate		
	$R^2$	GCV	%	$R^2$	GCV	%
All	0.862	0.0183		0.862	0.0183	
NO <sub>3</sub> *	0.857	0.0188	0.58	0.857	0.0188	0.58
WND†	0.844	0.0205	2.09	0.850	0.0198	1.39
MLD‡	0.768	0.0304	10.90	0.809	0.0252	6.15
SST§	0.660	0.0444	23.43	0.787	0.0281	8.70
Long, Lat	0.483	0.0670	43.97	0.710	0.0379	17.63
SOL	0.228	0.1005	73.55	0.767	0.0307	11.02

\* Nitrate.

† Wind speed.

‡ Mixed layer depth.

§ Sea surface temperature.

|| Solar radiation flux.

The whole-series spatio-environmental seasonal model is described first and then compared with the pre- and post-shift models to see divergences in this general pattern before and after the regime shift.

*Spatio-environmental model for the whole series*—This general annual-cycle model explained >85% of the total variance with all the covariates being significant, *see* Table 1 (left column). Stepwise deletion of covariates allowed us to estimate the variance contribution of the various covariates (Table 2). Nitrate, although significant, seems to contribute the least to the explained variance (<1%). Wind speed does not contribute much either (<2%), while the spatial term and light are the covariates that explain the most.

*Spatial pattern*: A combined spatio-environmental approach, as we chose here (formulation 1), allows us to account for a 'baseline' spatial distribution assuming no effect of the environment or season. Because month is not used as a predictor variable, it is only the additive effect of the various environmental variables upon this spatial pattern that gives rise to the seasonal cycle (*see* observations vs. predictions for the different month in the Web Appendix). As such, this spatial pattern may not have ever been observed in nature. It summarizes the variability left over by the selected environmental covariates and, therefore, can be used to explore the areas where this unexplained variance is more or less important (i.e., areas where the studied environmental factor satisfactorily explain most of the variance and areas where there must be other factors not included in the model). The average spatial distribution (Fig. 2) shows increasing levels towards the south-eastern coastal regions. The highest concentrations are found in the Southern Bight and the Wadden Sea, with a maximum centered at the German Bight, where it deviates +0.8 over the mean. The rest of the North Sea is characterized by a tongue of below-mean concentrations emanating from the northern North Sea in a southeasterly

direction to the coastal water just north of the Wadden Sea. This tongue-shaped region occupies about two-thirds of the total surface and is bounded by the slightly richer coastal areas off Scotland, England and Norway.

*Environmental effects*: The SOL has a very strong nonlinear effect on the PCI concentration (spanning the widest range; Fig. 2). Up to about 300 W m<sup>-2</sup> increasing light is associated with increasing PCI. Above this value increased light has no additional, or possibly even a negative, effect on PCI. Temperature (SST) has a nonlinear effect being positive up to about 11°C, above which increasing temperature does not lead to increased PCI. These saturation or decline effects for the upper ranges of SOL and SST could be indirectly summarizing the effect of other factors, such as nutrient depletion.

The effect of the MLD is strongly nonlinear, showing the highest PCI values at a MLD of around 50 m. There is a positive and almost linear effect of wind (WND; Fig. 2).

Nitrate did not have a strong statistical effect on the PCI seasonal cycle although entering significantly in the model. The highest PCI is found at intermediate nitrate concentrations.

*Preshift and post-shift 1988*—Summaries of the model results are shown in Table 1 (middle and right columns). The first and most noticeable change is the overall increase in the color mean level (intercept), which changed from 0.61 ( $\pm 0.01$  SE) to 0.92 ( $\pm 0.01$  SE.) after the regime shift, corresponding to an increase of >65%, but there have also been changes in the spatial distribution.

*Spatial pattern*: In the whole-series model, the geographic effect showed a mid-sea decrease compared to the coastal areas at both sides of the North Sea. In both the pre- and post-shift models, no such mid-sea decrease is shown by the geographic term (Fig. 3). Instead, the distribution of isolines is more fan-shaped, resembling a bunch of spokes coming out from Norway towards the south and south-

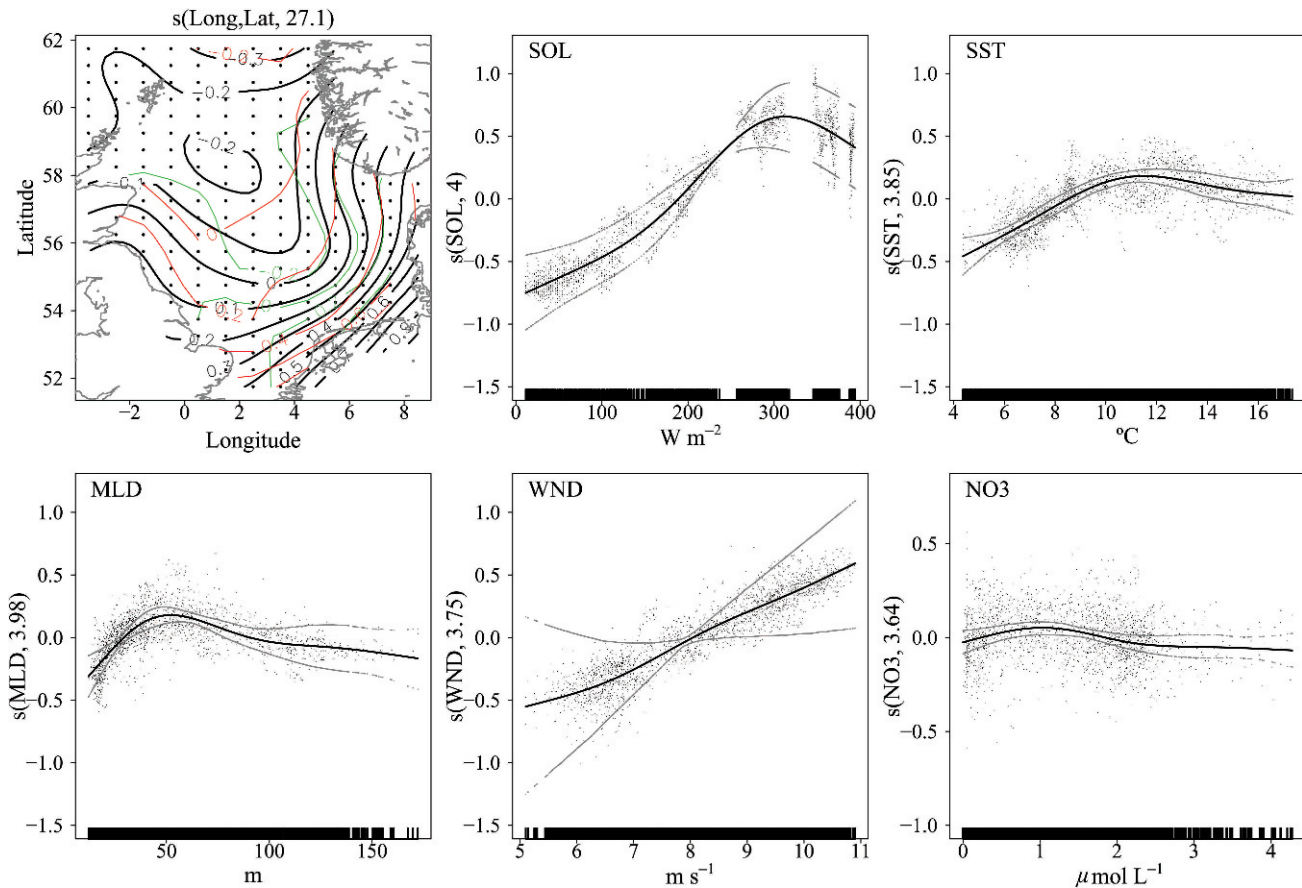


Fig. 2. Spatial and environmental effects. Spatial contours of the PCI as estimated by the whole-series spatio-environmental model. The small dots are the centers of the pixels shown in Fig. 1. The 95% upper (red) and lower (green) confidence intervals were calculated from bootstrapping. Partial plots of the environmental covariates selected by the whole-series seasonal model: Solar radiation (SOL), sea surface temperature (SST), mixed layer depth (MLD), wind speed (WND), and nitrate (NO<sub>3</sub>). The y-axis indicates the partial additive effect that the term on the x-axis has on the PCI. The numbers in parentheses on the x- and y-axes indicate the estimated degrees of freedom, which are also shown in Table 1. The 95% confidence intervals were calculated from bootstrapping and are shown in grey. Note that the scale of the x-axis for nitrate is different from the rest.

west, reflecting gradually lower color levels as one goes northwestwards in the North Sea. After 1988, this pattern is altered with a belt of low values (between the 0.8 isolines) extending from the western coast of Norway to Scotland. The area of minimum values thus seems to have moved south by 1–2° after 1988, from 61–62°N to ~58°N off Scotland to ~60°N off Norway (*see* 0.75 isoline).

**Environmental effects:** Regarding the effect of the environment, there are also slight differences before and after the shift (Fig. 4). Before 1988, increasing light led to increasing PCI even at the lowest light levels, while after 1988, the increase for the lower range was much lower (almost flat below 100 W m<sup>-2</sup>). On the other hand, above ~300 W m<sup>-2</sup>, increasing light prior to 1988 led to a sharper reduction in PCI than after 1988.

Temperature is the environmental variable whose effect changed the most. In the preshift period we found a positive effect of increasing SST up to about 10°C and a negative effect above this, while after 1988 the magnitude of the temperature effect is smaller and increasing SST

above about 10°C does not lead to reductions in PCI. It is worth noting that this variable is also the one that experienced the most pronounced change in range of values with a general increase (*see* x-axis ranges in Fig. 4).

The effect of wind was found to be plateau-shaped above 6 m s<sup>-1</sup> for the pre-1988 period (in contrast to the linear shape for the whole-series model), but did not enter significantly in the post-shift model.

Because comprehensive long-term MLD and nitrate data are not available on a broad spatial scale for the North Sea it was not possible to examine possible changes before and after the shift, as done with SST or SOL. Their effects in the pre- and post-shift models (not shown) did not vary much.

*Environmental changes after 1988*—To better interpret the adjustments found in the environmental regulation of phytoplankton color it is worth looking at the spatial changes in environmental conditions following the regime shift. Fig. 5 shows the difference between the annual mean post-shift and preshift conditions for the algal biomass index and the various environmental variables discussed

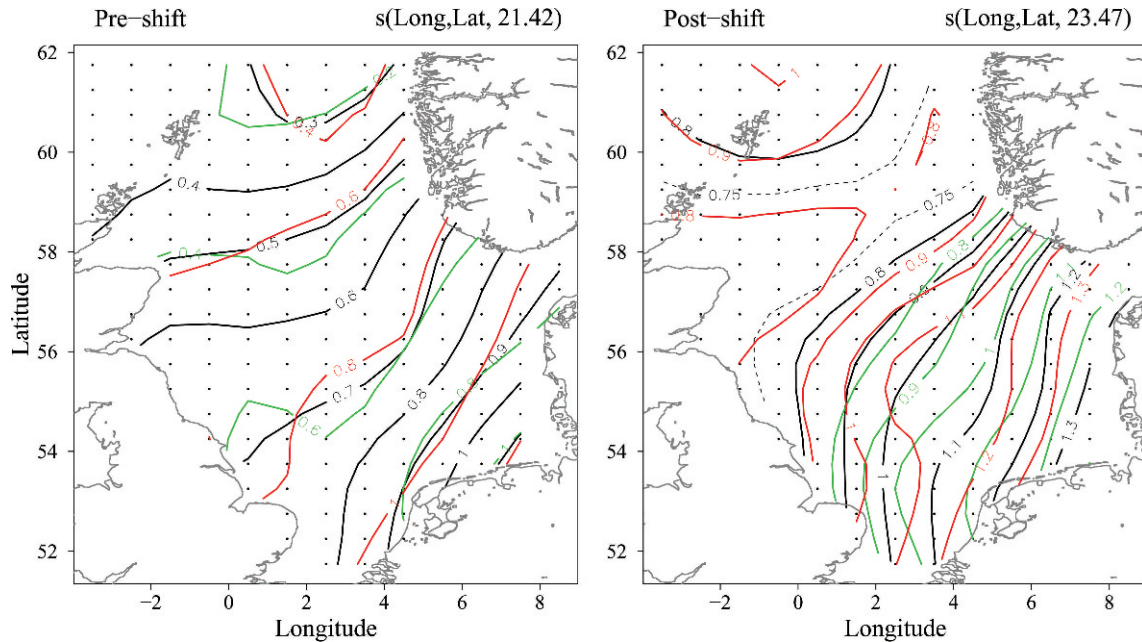


Fig. 3. Spatial effect - pre- and post-shift models. Spatial contours of the PCI concentration as estimated by the preshift (left) and post-shift (right) models. The value of the intercept has been added to the spatial effect in order to also show the increase in the mean level. The small dots are the centers of the pixels shown in Fig. 1. The numbers in parentheses on the top axes indicate the estimated degrees of freedom of the thin plate splines. The 95% upper (red) and lower (green) confidence intervals for the partial spatial effect were calculated from bootstrapping.

above. All the variables showed considerable changes, either in magnitude or in spatial pattern.

Overall, phytoplankton color increased all over the North Sea. However, this increase was much less intense off the coasts of Scotland and England, in particular between Aberdeen and the Humber estuary where the increase was below +0.3. Specifically, this area is characterized by an important decrease in the surface solar radiation (darkening) which could have contributed to this moderate increase (Fig. 5, bottom left plot). In fact, light is the only variable that diminished in intensity over a significant area after 1988. Both temperature and wind increased, although in a different spatial pattern. The changes in temperature show a clear north-south gradient, peaking in the Southern Bight where its increase was close to 1°C while wind speed increased mostly in the north and the south.

## Discussion

Although there have been >1000 publications using the CPR data (<http://www.sahfos.ac.uk/bibliography.htm>), there has been limited work on the evaluation of relationships between plankton dynamics and environmental variables (Edwards et al. 2002; Beaugrand 2004; Weijerman et al. 2005). The need to develop new methodologies to further explore this field, pointed out by Beaugrand et al. (2003), is currently growing with the increasing pressure for a more ecological approach to marine fisheries and environmental management.

Recently, McQuatters-Gollop et al. (2007) have used linear models to examine the relative importance of the

various hydro-meteorological variables on the phytoplankton biomass in the North Sea, while Raitsos et al. (2006) have used GAMs to explore the bloom size variation of coccolithophores in the subarctic North Atlantic. These two studies provide interesting results on the structuring effect of the marine environment. However, the spatial perspective has not been explicitly incorporated yet in the models.

In this study, we have explored the effect of the spatial position together with the environmental condition on the seasonal patterns of phytoplankton biomass in the North Sea via the framework of Generalized Additive Models (Hastie and Tibshirani 1990). One of the advantages of this nonparametric regression technique is that there is no need to a priori specify the functional form between the response and the explanatory variables. By using smoothers, we let the data tell us what this relationship (if any) looks like. This flexibility ensures an optimal empirical approach when aiming to infer causal relationships between two variables.

The results from our model show that the combination of a spatial term with the various physical and climatological variables (solar radiation, sea surface temperature, mixed layer depth, wind speed, nitrate concentration) successfully accounts for most of the variation in the North Sea of the subsurface spatial patterns in the seasonal cycle of the phytoplankton standing stock.

However, not all the variables have the same importance in driving the phytoplankton cycle. Light (SOL) was revealed as the most important environmental factor, well ahead of temperature or the depth of the mixed layer (Table 2). This covariate showed a strong nonlinear

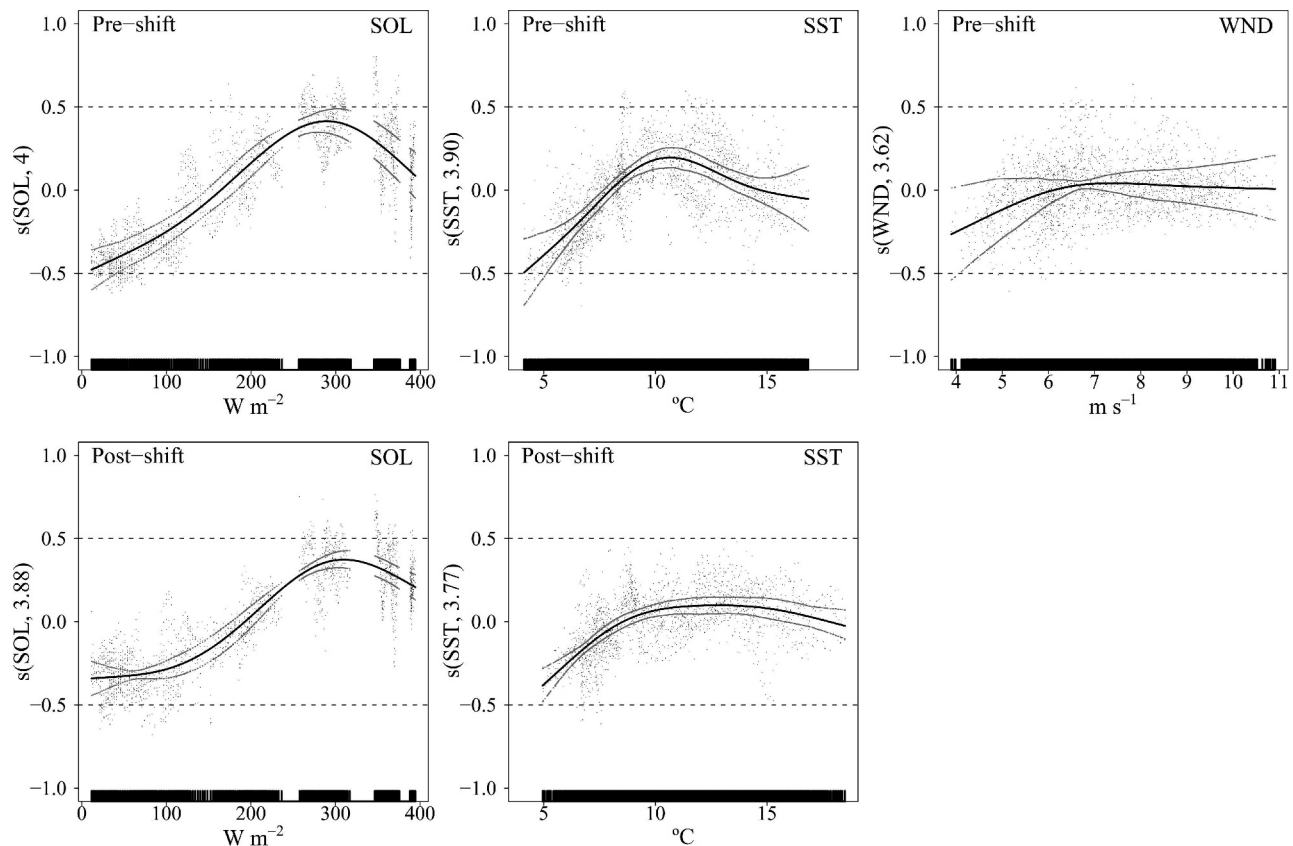


Fig. 4. Environmental effects - pre- and post-shift models. Partial residual plots of the environmental effects of solar radiation (SOL), sea surface temperature (SST), and wind speed (WND) from the preshift (upper row) and post-shift (lower row) models. WND does not appear in the post-shift model because it was not significant. The y-axis indicates the additive effect that the term on the x-axis has on the PCI. The numbers in parentheses on the y-axis indicate the estimated degrees of freedom, which are also shown in Table 1. The 95% confidence intervals were calculated from bootstrapping and are shown in grey. The horizontal dashed lines are included for visual comparison.

positive effect, with increasing values of light resulting in increasing PCI, until it exceeds  $350 \text{ W m}^{-2}$ . After this inflexion point its effect reverses (Fig. 2). These high values of light are found all over the North Sea from May to July, just at the time when the low PCI tongue reaches its maximal spatial extent, stretching all the way from the central to the northeastern North Sea. The rest of the year, increasing light leads to increasing PCI all over the North Sea.

Despite the recognized and well-known effect of light on phytoplankton growth (Sverdrup 1953; Letelier et al. 2004), its effect in relation to the regime shift has not yet been discussed (Beaugrand 2004). The main differences in the response of phytoplankton to solar radiation before and after the shift (Fig. 4) are found at the ends of the distribution ( $\text{SOL} < 100 \text{ W m}^{-2}$  and  $\text{SOL} > 350 \text{ W m}^{-2}$ ). For the lowest values (Oct–Feb), in the post-shift dynamics there is a much less intense positive response by the phytoplankton to increasing light levels compared to the clear effect before 1988. This attenuation is probably a result of the general increase of PCI and its reduced latitudinal spatial heterogeneity from October to February (see Web Appendix). Note that the partial plots refer to

deviations from the mean level, accounted for by the corresponding intercepts in Table 1.

On the other hand, the summer PCI increase in the coastal seas from Skagerrak to the Southern Bight could explain the reduced negative effect of light in the upper range. Based on a study of Secchi depth time series (Aarup 2002), McQuatters-Gollop et al. (2007) reported an improvement in water transparency since the mid-1980s. This reduction in turbidity, and subsequent increase in the light diffusion in the water column, could have led to a better use of available nutrients (Pätsch and Radach 1997), thus allowing a higher production. Moreover, because production is no longer restricted to the upper surface layers with highly variable light exposure, the need of the algae to reduce chlorophyll content to protect against very high radiation may have been reduced. Secchi depths are available for the North Sea since the 1970s. However, the data are temporally and spatially biased with the majority of samples taken in the Southern Bight, the Wadden Sea, the German Bight, and the Skagerrak area. This impedes the use of transparency as a covariate in our analysis approach and, therefore, its effects must be assessed indirectly.

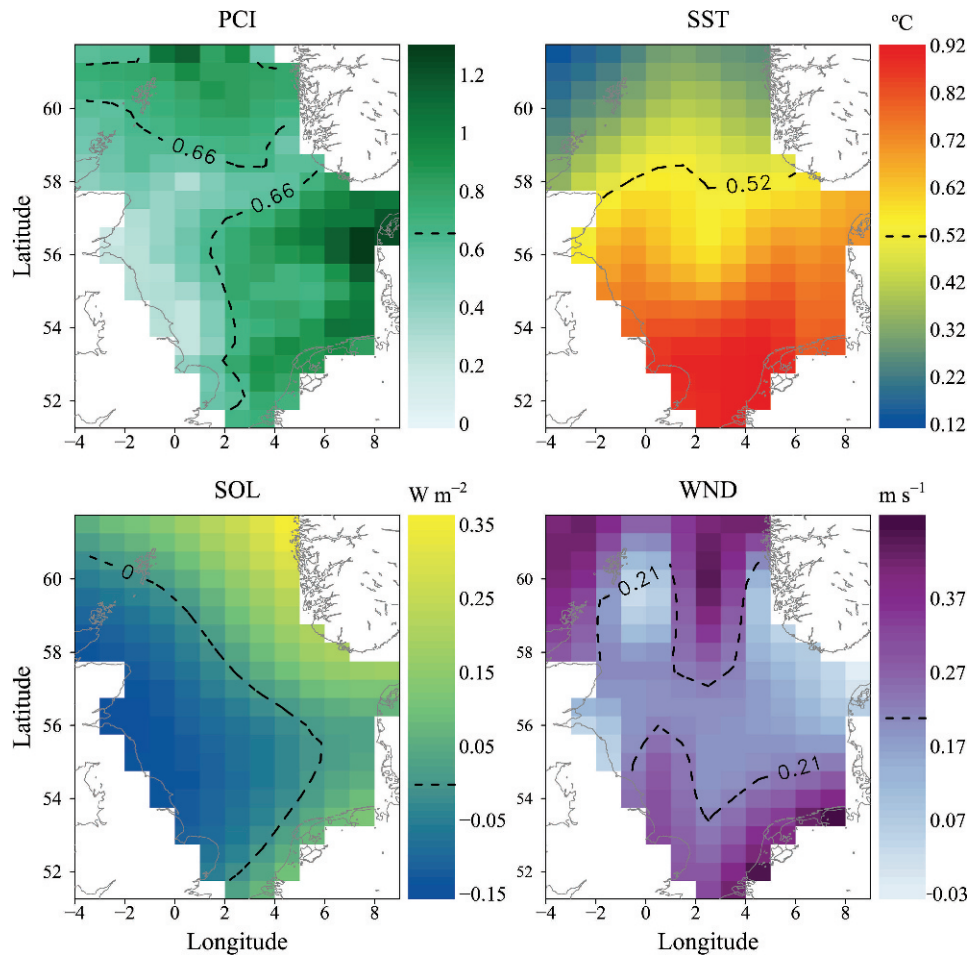


Fig. 5. Phytoplankton color and environmental anomalies after 1988. Fields of the anomalies (before and after 1988) over the North Sea for color (PCI), temperature (SST), light (SOL), and wind speed (WND). The maps show the difference between the annual average after and before 1988. The contour lines divide the whole area in regions of values below and above half of the total increase (for PCI, SST, and WND, which showed a net increase after 1988) and positive and negative anomalies (for SOL).

Overall, the amount of solar radiation reaching the surface of the water has decreased for half of the area of the North Sea after 1988 (Fig. 5). Interestingly, this darkened area, which would have experiencing more cloudiness in recent times, coincides roughly with the area showing the lowest increase in PCI after the shift (Fig. 5).

Temperature is the environmental variable that has changed the most in the long-term (from a range of values between 4.1–16.8°C to 4.9–18.5°C), showing on average an increase of almost 1°C in the Southern Bight and adjacent areas after 1988 (Fig. 5). This pronounced increase is even higher in some of the monthly anomalies, with the highest increase (1.5°C) occurring in May in the German Bight (data not shown). In terms of the phytoplankton response, it means that the lower tail of the SST partial plot no longer exists in the post-shift dynamics (Fig. 4, middle column). Moreover, the negative effect for the highest temperatures has disappeared such that the former Gaussian-shaped functional relationship becomes more like a saturation curve. A possible explanation for the attenuation of the negative effect of high temperatures, which could also be

argued for light, could be a change to a different summer flora which would be more tolerant to high light and temperature.

Wind speed (and derivatives, such as turbulence) showed a significant and positive rather linear effect in the whole-series model. The intervals of confidence turned out to be very wide, meaning that there is large uncertainty in the estimation of this effect. This may be a consequence of the negative correlation that exists between wind and other variables (mainly light) that would confound its effect with the rest of the environmental variables, although the positive effect in the whole-series model looks very strong. Accordingly, the increasing wind speed that occurred in the north and south of the North Sea after the 1980s may have contributed to the relatively high increase in the PCI that shows a similar spatial pattern.

Nitrate, although significant, has very little effect on the PCI while phosphate did not enter significantly. The statistically small effect of nutrients suggests that these are not generally limiting factors for phytoplankton in the North Sea. This result is in good agreement with the study

by McQuatters-Gollop et al. (2007), who concluded that the long-term increase in phytoplankton is unconnected to nutrients. The authors showed how nutrient concentration in the North Sea has been declining since the early 1980s while phytoplankton biomass has continued to increase. The southern half of the North Sea shows an average nutrient concentration that is much higher than the oceanic-driven northern half. In the shallow areas below 56°N nitrate can reach concentrations well above 50  $\mu\text{mol L}^{-1}$ , even in summer. Winter nutrient dynamics only resemble those of the open ocean in the northern and central regions. In these regions nutrients should be important, with summer depletion limiting phytoplankton growth. It is possible that due to a stronger seasonality, the dynamics of nutrients are well-captured by the other environmental variables, such as temperature or light.

The highly significant spatial effect (Fig. 2) indicates that the high phytoplankton densities occurring in the southeastern coastal regions are not fully explainable through the other explanatory variables retained in the model. A combination of a weak summer stratification and year-round increased nutrient content due to tidal mixing, shallowness, and river discharges may be responsible for the higher algal density in this area. It is worth noting that this spatial structure reproduces the tidal-mixing field estimated by Pingree and Griffiths (1978). This was used as a covariate and was only significant when the location was not entered, indicating that both variables carry similar information. On the other hand, observations by CPR analysts suggest that detrital material (which may or may not be primarily phytoplanktonic in origin) is frequently found in southern North Sea samples. The samples often have a brown or greenish color, and a high PCI, but actual cell counts are low (Batten et al. 2003b). The presence of particulate and/or dissolved organic matter is also an issue when using telemetry because Chl *a* cannot readily be distinguished from them (Raitsois et al. 2006). Any of these proposed explanations (either the interplay of other physical or environmental processes leading to higher than average PCI or the 'contamination' by detritus) or a combination of both are accounted for by the spatial term.

The North Sea regime shift, consisting of a rapid increase followed by a consistently high level of phytoplankton biomass, has been described elsewhere (Beaugrand 2004). However, the spatial changes that accompanied the shift have not been investigated. Apart from the total increase, which agrees well with the 60% reported by Raitsois et al. (2005); the main difference that arises from the comparison between the pre- and post-shift contours is that the spatial pattern passed from a unimodal to a bimodal distribution after 1988 (Fig. 3). The common southern local maximum, located in the German Bight, is accompanied now by another local maximum east of the Shetland Isles. The inter-regime increase at this second center of gravity has been of >0.4 units while in the German Bight it was ~0.3. In the central regions of the North Sea the increase has been around 0.2 units.

The improvement in transparency and the increase in temperature, light, and wind in the southeastern North Sea

have probably contributed to the increase in the algal biomass in this region. In contrast, the development of a maximum in the northern North Sea requires a different explanation because transparency is not an issue in the open sea and the warming has been little compared to the south (Fig. 5). Solar radiation and wind show up as the environmental variables that may have contributed the most because it is in this region where the highest deviations are found.

To further investigate the effect of the two most important environmental variables discussed above (SOL and SST), a simplified formulation of the pre- and post-shift models was run. In these new models, only the geographical term and either SOL or SST were entered to exclude the partial effects of the rest of the environmental variables (as opposed to the results shown previously). The predictions of the model against the corresponding environmental variable are shown in Fig. 6 with different colors for different regions of the North Sea. Apart from some of the aspects commented on above, it is worth noting that in the post-shift dynamics some of the transects reach a plateau towards the south (represented by blue and red circles) for increasing values of light but particularly for increasing values of temperature and in the north end of the transects (yellow and green circles), the range of PCI values for varying SST and SOL has shrunk so that the spatial gradient in this area is less pronounced now. It seems that after the shift (Fig. 6, bottom plot), whereas in the central North Sea increasing light or temperature can still lead to increasing PCI (by displacing upwards along the range covered by the grey open circles), in the south and north there are other factors that hinder this increase (filled circles). These limiting factors might be nutrients in the north during summer, where an increase in wind speed could still enhance the PCI; however, in the south, nutrients are not considered to be limiting and the tidal forcing keeps the waters mixed year-round. This region has experienced the most pronounced warming of the whole sea since the late 1980s and also moderate and pronounced increases in light and wind respectively. The saturation pattern displayed by the stations in this area suggests that the system might have reached here its new carrying capacity, which is probably still limited by turbidity.

By analyzing the unique PCI data from the CPR survey, using a spatial nonparametric approach, we show how surface phytoplankton biomass varies seasonally and spatially in relation to environmental conditions. Our results highlight the different nonlinear responses to the various environmental factors as well as the most important effects of light and temperature. Increasing levels of temperature, wind speed, and light seem to have contributed to the new phytoplankton regime, established since 1988. The present state may have reached a maximum in the southernmost areas where increasingly favorable conditions (out of those studied here) did not lead to a significant increase of phytoplankton biomass. In contrast it is expected that the northern North Sea will continue to respond positively to a warmer, brighter, and windier future if current trends are maintained.

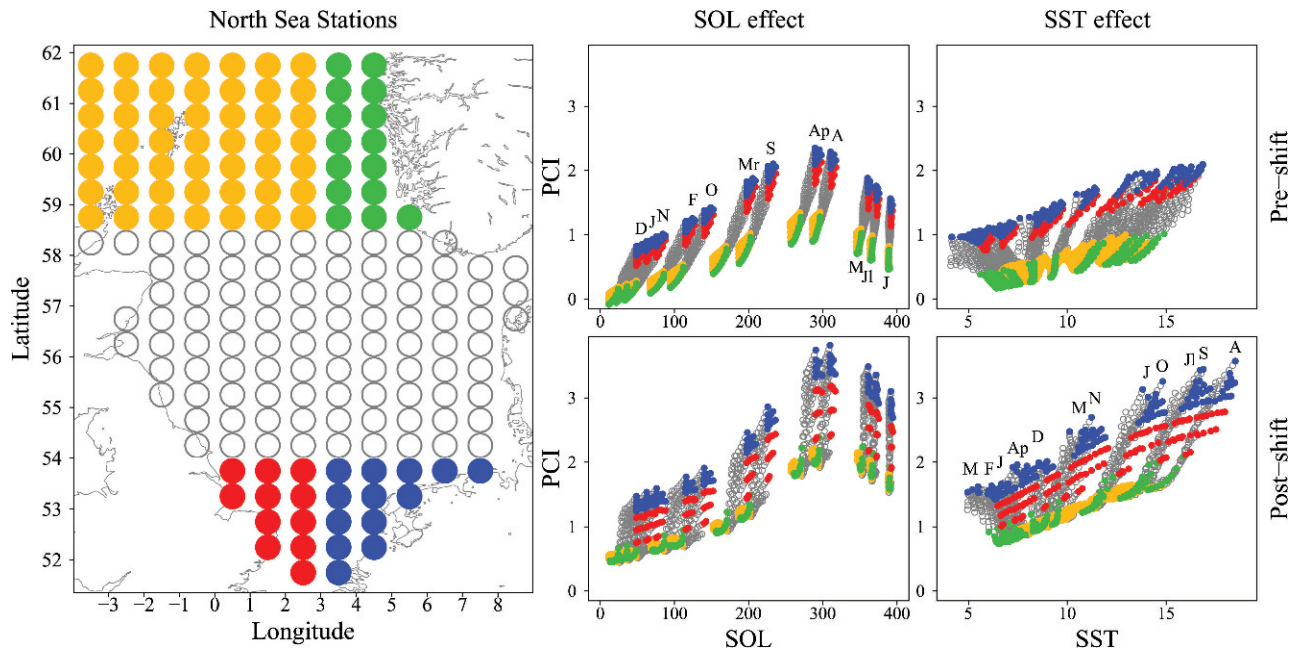


Fig. 6. Light and temperature effects. Results from simplified pre- and post-shift models (including only the spatial effects and either SOL or SST as environmental covariates). Varying colors have been used in order to regionally identify the different responses (map, left column). The PCI values predicted by the model against the environmental variable that was used as predictor, either SOL or SST, are shown in the middle and right column respectively for the pre- (upper panel) and post-shift models (lower panel). The small letters stand for the different months.

## References

- AARUP, T. 2002. Transparency of the North Sea and Baltic Sea—a Secchi depth data mining study. *Oceanologia* **44**: 323–337.
- BATTEN, S. D., AND OTHERS. 2003a. CPR sampling: The technical background, materials and methods, consistency and comparability. *Prog. Oceanogr.* **58**: 193–215.
- , A. W. WALNE, M. EDWARDS, AND S. B. GROOM. 2003b. Phytoplankton biomass from continuous plankton recorder data: An assessment of the phytoplankton color index. *J. Plankton Res.* **25**: 697–702.
- BEAUGRAND, G. 2004. The North Sea regime shift: Evidence, causes, mechanisms and consequences. *Prog. Oceanogr.* **60**: 245–262.
- , F. IBANEZ, AND J. A. LINDLEY. 2003. An overview of statistical methods applied to CPR data. *Prog. Oceanogr.* **58**: 235–262.
- COLEBROOK, J. M., AND G. A. ROBINSON. 1965. Continuous plankton records: Seasonal cycles of phytoplankton and copepods in the north-eastern Atlantic and North Sea. *PSZNI: Mar. Ecol.* **6**: 123–139.
- DAVISON, A. C., AND D. V. HINKLEY. 1997. *Bootstrap methods and their applications*, 8th ed. Cambridge Univ. Press.
- EDWARDS, M., G. BEAUGRAND, P. C. REID, A. A. ROWDEN, AND M. B. JONES. 2002. Ocean climate anomalies and the ecology of the North Sea. *Mar. Ecol. Prog. Ser.* **239**: 1–10.
- , P. REID, AND B. PLANQUE. 2001. Long-term and regional variability of phytoplankton biomass in the Northeast Atlantic (1960–1995). *ICES J. Mar. Sci.* **58**: 39–49.
- HASTIE, T., AND R. J. TIBSHIRANI. 1990. *Generalized additive models*. Chapman & Hall.
- INTERGOVERNMENTAL PANEL ON CLIMATE CHANGE. 2007. Summary for policymakers. In B. Metz, O. R. Davidson, P. R. Bosch and R. Dave and L. A. Meyer [eds.], *Climate change 2007: Mitigation. Contribution of working group III to the fourth assessment report of the Intergovernmental Panel on Climate Change*. Cambridge Univ. Press. Available from [http://www.mnp.nl/ipcc/docs/FAR/Approved%20SPM%20WGIII\\_0705rev5.pdf](http://www.mnp.nl/ipcc/docs/FAR/Approved%20SPM%20WGIII_0705rev5.pdf).
- KALNAY, E., AND OTHERS. 1996. The NCEP/NCAR 40-year reanalysis project. *Bull. Am. Met. Soc.* **77**: 437–471.
- LETELIER, R. M., D. M. KARL, M. R. ABBOTT, AND R. R. BIDIGARE. 2004. Light driven seasonal patterns of chlorophyll and nitrate in the lower euphotic zone of the North Pacific Subtropical Gyre. *Limnol. Oceanogr.* **49**: 508–519.
- MAMMEN, E. 1993. Bootstrap and wild bootstrap for high dimensional linear models in resampling. *Ann. Stat.* **21**: 255–285.
- MCQUATTERS-GOLLOP A., D. E. RAITOS, M. EDWARDS, AND M. J. ATTRILL. 2007. A long-term chlorophyll data set reveals regime shift in North Sea phytoplankton biomass unconnected to nutrient trends. *Limnol. Oceanogr.* **52**: 635–648.
- MONTÉGUT, C. D. B., G. MADEC, A. S. FISCHER, A. LAZAR, AND D. IUDICONE. 2004. Mixed layer depth over the global ocean: An examination of profile data and a profile-based climatology. *J. Geophys. Res.* **109**: C12003, doi:10.1029/2004JC002378.
- NEUWIRTH, E. 2007. RColorBrewer: ColorBrewer palettes. R package version 1.0-1 [accessed 2008 Dec 08]. Available from: [http://www.personal.psu.edu/cab38/ColorBrewer/ColorBrewer\\_intro.html](http://www.personal.psu.edu/cab38/ColorBrewer/ColorBrewer_intro.html).
- PÄTSCH, J., AND G. RADACH. 1997. Long-term simulation of the eutrophication of the North Sea: Temporal development of nutrients, chlorophyll and primary production in comparison to observations. *J. Sea Res.* **38**: 275–310.
- PINGREE, R. D., AND D. K. GRIFFITHS. 1978. Tidal fronts on the shelf seas around the British Isles. *J. Geophys. Res.* **83**: 4615–4622.
- R DEVELOPMENT CORE TEAM. 2007. *R: A language and environment for statistical computing*. R Foundation for Statistical Computing.

- RAITSOS, D. E., S. J. LAVENDER, Y. PRADHAN, T. TYRRELL, P. C. REID, AND M. EDWARDS. 2006. Coccolithophore bloom size variation in response to the regional environment of the subarctic North Atlantic. *Limnol. Oceanogr.* **51**: 2122–2130.
- , P. C. REID, S. J. LAVENDER, M. EDWARDS, AND A. RICHARDSON. 2005. Extending the SeaWiFS chlorophyll data set back 50 years in the northeast Atlantic. *Geophys. Res. Lett.* **32**: L06603, doi:10.1029/2005GL022484.
- REID, P. C., M. F. BORGES, AND E. SVENDSEN. 2001. A regime shift in the North Sea circa 1988 linked to changes in the North Sea horse mackerel fishery. *Fish. Res.* **50**: 163–171.
- , J. M. COLEBROOK, J. B. L. MATTHEWS, AND J. AIKEN. 2003. The continuous plankton recorder: Concepts and history, from plankton indicator to undulating recorders. *Prog. Oceanogr.* **58**: 117–173.
- , M. EDWARDS, H. G. HUNT, AND A. J. WARNER. 1998. Phytoplankton change in the North Atlantic. *Nature* **391**: 546.
- STENSETH, N. C., AND OTHERS. 2006. Seasonal plankton dynamics along a cross-shelf gradient. *Proc. Royal. Soc. B* **273**: 2831–2838, doi:10.1098/rspb.2006.3658.
- SVERDRUP, H. V. 1953. On conditions for the vernal blooming of phytoplankton. *J. Cons. Perm. Int. Explor. Mer.* **18**: 287–295.
- VEZZULLI, L., P. S. DOWLAND, P. C. REID, AND E. K. HYLTON. 2007. Gridded database browser of North Sea plankton, version 1.1: Fifty four years (1948–2001) of monthly plankton abundance from the Continuous Plankton Recorder (CPR) survey. Sir Alister Hardy Found [accessed 2008 Dec.]. Available from <http://cpr.cisnr.org>.
- WEIJERMAN, M., H. LINDEBOOM, AND A. F. ZUUR. 2005. Regime shifts in marine ecosystems of the North Sea and Wadden Sea. *Mar. Ecol. Prog. Ser.* **298**: 21–39.
- WOOD, S. J. R. 2000. Modelling and smoothing parameter estimation with multiple quadratic penalties. *J. R. Stat. Soc. B* **62**: 413–428.
- WOOD, S. N. 2006. Generalized additive models: An introduction with R. Chapman & Hall/CRC.

*Edited by: Robert R. Bidigare*

*Received: 25 March 2008*

*Accepted: 29 September 2008*

*Amended: 02 November 2008*